J Food Sci Technol (April 2018) 55(4):1314–1324
https://doi.org/10.1007/s13197-018-3042-0

ORIGINAL ARTICLE

Production and characterization of vitamin D_3 loaded starch nanoparticles: effect of amylose to amylopectin ratio and sonication parameters

Elham Hasanvand[1] · Milad Fathi[2] · Alireza Bassiri[3]

Revised: 3 January 2018 / Accepted: 15 January 2018 / Published online: 6 February 2018

Abstract Two types of starches with different amylose to amylopectin ratios were used for the production of vitamin D_3 loaded nanoparticles and effects of starch type, sonication time and temperature on physicochemical properties of nanocarriers were investigated. Both high amylose corn and potato starches nanocarriers had granular structure with particle size ranging from 32.04 to 99.2 nm and the encapsulation efficiency ranging from 22.34 to 94.8%. The results showed that potato starch nanoparticles had larger size, higher zeta potential, encapsulation efficiency and encapsulation load and lower polydispersity index values in comparison to high amylose corn starch nanoparticle. Increase in sonication time reduced the size of nanoparticles in both starch types and decreasing temperature led to reduction of particle size and increase of zeta potential. Physicochemical features of nanocarriers were analyzed by Fourier transform-infrared spectroscopy, X-ray diffraction and differential scanning calorimetry. The results indicated that vitamin D_3 is well incorporated in carriers and ultrasonic treatment led to increase of hydrocarbon chain that resulted in van der Waals and hydrogen bonds of vitamin D_3 with the potato starch and greater thermal stability.

✉ Milad Fathi
mfathi@cc.iut.ac.ir

[1] Department of Food Science and Technology, Institute of Agricultural Engineering, Iranian Research Organization for Science and Technology (IROST), Tehran, Iran

[2] Department of Food Science and Technology, College of Agriculture, Isfahan University of Technology, Isfahan 84156-83111, Iran

[3] Department of Food Science and Technology, Institute of Chemical Engineering, Iranian Research Organization for Science and Technology (IROST), Tehran, Iran

Keywords Amylose to amylopectin ratio · Nanoparticles · Starch · Vitamin D

Introduction

Encapsulation of food bioactives is one of the best ways to increase sustainability, bioavailability and apparent solubility. Nanoencapsulation of poorly water-soluble compounds, leads to enhancement of transparency, stability and solubility which consequently increases absorption in the gastrointestinal tract (Merisko-Liversidge and Liversidge 2008). Vitamin D is a fat-soluble ingredient with important roles in calcium and phosphorus metabolism and prevention of osteoporosis in adults and rickets in children. However, it is sensitive to light, oxygen and heat (Pettifor and Prentice 2011), therefore vitamin D preservation is necessary before its application in food systems. Moreover, this vitamin is a highly lipophilic molecule that limits its use in aqueous solutions. Instead, it needs to be incorporated into an appropriate colloidal system prior to dispersion. In order to explore targeting purpose and also improve bioavailability, it is necessary to review carrier systems (Almouazen et al. 2013). Zein nanoparticles coated with carboxymethyl chitosan (CMCS) were prepared to encapsulate vitamin D_3 and calcium was added to cross-link CMCS to achieve thicker and denser coatings (Luo et al. 2012). Another carrier system of vitamin D_3 was complex nanoparticles of carboxymethyl chitosan (CMCS) and soy protein isolate (SPI) by a simple ionic gelation method (Teng et al. 2013). Carbohydrates possess high biodegradability, biocompatibility, active groups to interact with hydrophobic and hydrophilic compounds and high heat stability which make them as suitable shell to entrap sensitive bioactives. Starch, the second most abundant

biopolymer in the nature, is low cost, non-toxic and resistant to varying degrees of enzymatic hydrolysis and therefore it is a good candidate for the production of food delivery systems (Araújo et al. 2004). It is hydrophilic biopolymer consisted of linear molecule (amylose) with glycoside links $\alpha - D\ (1 \rightarrow 4)$ and branched molecule (amylopectin) with glycoside links $\alpha - D\ (1 \rightarrow 4)$ and $(1 \rightarrow 6)$. Amylose to amylopectin ratio varies in different starch sources (Davis et al. 2003) and affects properties and functionalities of starch. Amylose has a hydrophobic cavity which provides the possibility of inclusion of small hydrophobic molecules therein (Godet et al. 1995). Previous studies showed formation possibility of complexes of starch and fatty acids (Bhosale and Ziegler 2010) as well as aromas and flavor (Heinemann et al. 2005) and vitamin D (Hasanvand et al. 2015).

Several methods have been reported to produce nanoparticles. Ultrasound is an effective technique for reducing the size of particles in the nano range by cavitation phenomenon (Tischer et al. 2010). The energy provided by cavitation approximately is about 10–100 kJ/mol that is equivalent to hydrogen bonds energy Hydrogen bond breakage leads to reduction of size and polydispersity index of nanoparticles (Tischer et al. 2010). Effects of high intensity and low frequency ultrasound treatment on potato starch granules at low temperature (5 °C) for 30 min were studied. The results showed this treatment caused damage of the starch granules and in some cases, their disjoint (Zuo et al. 2012).

The aims of this study were application of high amylose corn starch and potato starch as encapsulating shells for vitamin D_3, and investigation of effects of temperature and sonication time on physicochemical properties of nanocapsules.

Materials and methods

Materials

High amylose corn starch (HACS) with 70% amylose and potato starch as a low amylose starch were purchased from Sigma–Aldrich (St. Louis, MO, USA) and Merck (Germany), respectively. Vitamin D_3 was obtained from DSM (Neuf. France). Potassium hydroxide, n-Hexan and all other chemicals were of analytical grade and obtained from Merck (Darmstadt, Germany). Double distilled water was used for preparing samples.

Production of vitamin D_3 loaded nanocapsules

HACS solution (2% w/v) in 0.1 M KOH and potato starch solution (2% w/v) in distilled water were preheated at 80 ± 1 °C for 30 min and cooled to 30 ± 1 °C. One milliliter of VD_3 solution in pure ethanol (2.5% w/v) was added dropwise into 50 ml starch solution with mild stirring for 1 min. Probe ultrasound generator (Misonix, S-4000, USA) with a diameter of 19 nm was located at depth of 1 cm below the surface. Sonication was performed at frequency of 24 kHz and power of 450 W for 5 and 10 min. The process was stopped for 10 s intervals to inhibit temperature increase. The obtained suspension was frozen at-18 °C, dried by freeze dryer (Christ ALPHA1-4LD Plus, Germany) and ground into fine powder for future analyses. Table 1 shows the sample codes of different nanocarriers.

Encapsulation efficiency (EE) and encapsulation load (EL)

Encapsulation efficiency describes the fraction of encapsulated compound incorporated into the nanoparticles compared to the total amount of encapsulant that was initially added (Eq. 1). Encapsulation load is the mass fraction of loaded composition compared to synthesized nanoparticles, in the other word expresses the mass ratio of core to total nanoparticle (Eq. 2). The encapsulation efficiency of VD-loaded nanoparticles was calculated by a previously reported method (Luo et al. 2012). Calibration curve of vitamin D in hexane (concentration in terms of absorption) was plotted and data were transformed in Vitamin D_3 weight. Ten milligrams of the freeze-dried nanoparticles powder was washed with 5 ml n-hexane and the suspension was filtrated through a Whatman No. 1 filter paper. The filtrate was subjected to spectrophotometric measurement at wavelength of 264 nm with a LAMBDA 25 UV/VIS spectrophotometer (Perkin Elmer, Waltham, Massachusetts). This procedure was repeated until the absorption of last filtrate became zero. All filtrates were combined and its absorbance was measured for determination of free VD_3. Nanoparticles remained after filtration were dried and weighed.

$$EE(\%) = 100 - \left(\frac{Weight\ of\ free\ vitamin\ D}{Weight\ of\ initial\ vitamin\ D\ used} \times 100\right) \quad (1)$$

$$EL(\%) = \frac{Weight\ of\ vitamin\ D\ loaded\ in\ nanoparticles}{Weight\ of\ nanoparticles} \times 100 \quad (2)$$

Particle size, polydispersity index and zeta potential

The average particle size, polydispersity index (PDI) and zeta potential of vitamin D_3 loaded nanoparticles were

Table 1 Sample code and compare means of interaction of temperature, time and starch type on size, zeta potential, PDI, EE and LE of nanoparticles

Starch	Temp (°C)	Time (min)	Sample code	Size	Zeta potential	PDI	LE (%)	EE (%)
Corn	0	5	CSN-0-5	38.3 ± 0.66^{b}	-19.6 ± 0.4^{d}	0.33 ± 0.25^{d}	22.34 ± 1.2^{g}	1.09 ± 2.3^{e}
		10	CSN-0-10	32.04 ± 0.45^{a}	-17.59 ± 0.46^{e}	0.343 ± 0.37^{d}	61.07 ± 1.4^{d}	2.98 ± 1.8^{c}
	15	5	CSN-15-5	60.18 ± 1.2^{f}	-8.49 ± 0.73^{h}	0.299 ± 0.35^{c}	28.44 ± 0.98^{f}	2.04 ± 1.9^{d}
		10	CSN-15-10	40.33 ± 1.4^{c}	-13.58 ± 0.83^{f}	0.382 ± 0.67^{e}	$46.7 \pm {}^{e} 0.76$	2.22 ± 2.5^{d}
Potato	0	5	PSN-0-5	66.1 ± 0.87^{g}	-33.39 ± 1.3^{a}	0.214 ± 1.8^{b}	87 ± 1.7^{b}	3.67 ± 1.7^{c}
		10	PSN-0-10	54.9 ± 0.56^{d}	-31.83 ± 1.5^{b}	0.173 ± 0.29^{a}	94.71 ± 2.1^{a}	5.07 ± 0.18^{a}
	15	5	PSN-15-5	99.2 ± 0.91^{h}	-22.96 ± 1.7^{c}	0.208 ± 0.9^{b}	94.8 ± 1.4^{a}	5.8 ± 2.1^{a}
		10	PSN-15-10	57.1 ± 1.1^{e}	-10.98 ± 0.88^{g}	0.164 ± 0.8^{a}	85.9 ± 1.6^{c}	4.37 ± 2.1^{b}

Different letters show significant differences in 95% confidence

Sample code is illustrated as x–y–z in which x, y and z mean starch sources, temperature (°C) and time (min), respectively

determined by dynamic light scattering (DLS) (90Plus Nanoparticle Size Analyzer, Brookhaven Instruments). Size measurements were performed at a fixed angle of 90° using volume distribution. Poly dispersity index (PDI) measures the size distribution of the nanocarriers. The lower the PDI the narrower the size distribution. Zeta potential which is an indicator of surface charge was measured based on mean electrostatic mobility. All measurements were repeated three times for each sample.

Morphology characterization

The morphology of VD_3-loaded nanoparticles was observed by Field Emission Scanning Electron Microscopy (MIRA3, TESCAN, Czech Republic). Drib of the nanoparticle dispersions was dripped and cast-dried on an aluminum pan, which was cut into appropriate sizes. The samples were then coated with a thin layer (< 20 nm) of gold using a sputter coater (Hummer XP, Anatech, CA, USA).

Turbidity measurement

Turbidity of samples was indicated by spectrophotometer (Perkin Elmer, Waltham, Massachusetts). Sample absorbance measured at wavelength of 600 nm and using distilled water as a control sample (Esfanjani et al. 2015).

Fourier transform infrared spectroscopy

Fourier-transform infrared spectroscopic studies were performed in transmission mode using Philips PU9624 FTIR spectrometer. The FTIR spectra of pure materials and physical mixtures were compared with VD_3 loaded nanoparticle. Tablets comprising of 300 mg of KBr and 2 mg of samples were prepared for FTIR tests. Spectra were obtained at 4 cm^{-1} of resolution from 4000 to 400 cm^{-1}.

X-ray diffraction analysis

The crystallographic structural analysis was carried out by X-ray diffractometer (XRD- EQuinox 3000, INEL, France). The operating conditions were Cu K-alpha-1 radiation (0.154 nm), under voltage of 40 kV and current of 30 mA. Approximately 200 mg of sample powders were loaded in an aluminum plate and scanned over the range –10 to 118 Bragg angles in steps of 0.02° per second.

Thermal analysis

Thermal transition properties of pure materials, physical mixture of starch and vitamin D_3 with weight ratio similar to formulations and VD_3 loaded nanocarriers were measured by a differential scanning calorimeter (DSC -60, Shimadzu, Tokyo, Japan). The instrument was calibrated with indium and an empty pan was used as reference. The samples were scanned from 0 to 330 °C at 10 °C/min.

Statistical analysis

All experiments were performed at least in three replications, and average values were reported. Statistical analysis was carried out using SPSS 16 software. Data were subjected to analysis of variance, and means were compared using "Duncan" test at 5% significant level.

Results and discussion

Size, zeta potential, particle distribution index (PDI), EE and EL

Analysis of variance showed that sonication time had significant effects ($p < 0.005$) on size, zeta potential, particle distribution index (PDI) and EL. All studied features except PDI were significantly ($p < 0.05$) affected by

temperature. The influences of type of starch on all factors were significant ($p < 0.05$).

Effect of time at different levels of starch and temperature

As seen in Table 1, an increase in duration of the ultrasound treatment led to reduction of size of nanoparticles in both starch types, while reducing size during 10 min treatment is greater than 5 min. Similar results were reported for particle sizes reduction of waxy maize and standard maize starch nanoparticle from several micron meters to 100–200 nm in results of increase of sonication time for 75 min. By increasing ultrasonication time, surface of the granules appeared to be progressively broken down, eroded and complete disintegration of starch granules into nano-sized particles (Haaj et al. 2013). Study of simple effect of time at different levels showed that increase in duration of treatment caused exposure of solid starch particles to bubble explosion for longer time, which led to rapid flow of liquid to the solid particles, severe collisions and fragmentation of particle which finally caused a reduction in particle size (Patist and Bates 2008). The efficiency of chemical reactions increased with increasing sonication time that contributed the increase of interaction of vitamin D and starch and thereby increasing the values of EE and EL.

Effect of temperature at different levels of starch and time

The different effects of temperature in the low frequency ultrasound were explained by four important parameters affected by temperature. Increasing the temperature of the liquid (1) reduce cavitation energy (2) decrease cavitation threshold limit (3) reduce quantity of the dissolved gas and (4) increase vapor pressure. In low ultrasound frequency raising temperature led to increase of coalescence of the bubbles, and lose of activity of bubbles. Therefore reduction in the temperature of the solution results in increase of the rate of chemical reactions (Jiang et al. 2006).

The results showed that decreasing temperature led to reduction of particle size and increase of zeta potential. However, the EE, EL did not change significantly. Investigation of the effect of two different temperatures on particle size of corn starch nanoparticles [treated for 10 min at 0 °C; (CSN-0-10) and (CSN-15-10)] showed that the size increased (40.33 nm) by increasing temperature to 15 °C. This trend was also observed for 5 min treatment of potato starch nanoparticles, which is similar to results reported by Rao et al. 2005 who prepared monodisperse and uniform-size silica nanoparticles using ultrasonication by sol–gel process and studied effect of temperature on particle size. Ultrasonic waves in liquid create electrical charge and plasma effects and great cycles of cooling–heat ($> 10^9$K/s) (Suslick 1988). Water molecules under such extreme conditions undergo thermal dissociation to yield H^+ and HO^- radicals (Makino et al. 1983). The results showed that application of lower temperature led to enhancement of electric charges. It causes an increase in zeta potential (Table 1) and therefore enhancement of solution stability during storage (Üner 2006).

Effect of type of starch at different levels of time and temperature

Potato starch nanoparticles had larger size, higher zeta potential, EE and EL (Table 1) and lower PDI values in comparison to high amylose corn starch ($p < 0.05$). Amylose to amylopectin ratio is one of the important factors affecting particle size distributions of the granules and, therefore, size of nanoparticles. The difference in size is likely affected by the amounts of amylose molecules which were available for interaction with vitamin D. Amylose to amylopectin ratio also had influence on ultrasound efficiency of destruction of starch molecular structure. Moreover, increase of load of vitamin D_3 as a hydrophobic vitamin with high molecular volume in potato starch nanoparticle (with higher percentage of amylopectin) is due to an increase in the size of particles compared with high amylose corn starch nanoparticle. Nano-complexes of beta-lactoglobulin-pectin showed nearly 5 times increase in particle size by vitamin D loading (Ron et al. 2010). Loading alpha-tocopherol to beta lactoglobulin led to increase of particle size from 183 to 314 nm (Relkin and Shukat 2012). Potato starch nanoparticles have PDI value less than 0.22 that indicated their narrower size distribution. PSN-0-10 had the highest EE and EL and the smallest size (EE of 94.71%, EL over 5%, particle size less than 55 nm and PDI about 0.17). The interaction of vitamin D_3 with potato starch that had higher amylopectin percentage, was significantly ($p < 0.05$) higher than high amylose corn starch. Amylose is able to form inclusion complexes with a variety of ligands that parts of hydrophobic ligands trapped in hydrophobic helix cavity of amylose. This amylose is called V-type amylose (Gökmen et al. 2011). Previous studies showed that if XRD results confirmed that encapsulation of hydrophobic compound in starch was not due to formation a complex with amylose helix, the main reason of encapsulation would be the interaction with amylopectin (Putseys et al. 2010). The reason of encapsulation of massive molecules by multi-ring compounds, is formation of hydrogen bonds between starch and the bioactive compound and is not due to creation of inclusion complexes (Boutboul et al. 2002). However, despite extensive studies on formation of complexes with amylose, very few works have been reported on interaction of hydrophobic compounds with amylopectin (Guichard 2002).

The results of this study suggests applying of potato starch with greater amylopectin percent to interact with vitamin D, as well as the use of low temperatures in the high intensity and low frequency ultrasound for 10 min.

Morphology

To study morphology of VD_3-loaded starch nanoparticles, FE-SEM observations were performed (Fig. 1). Images showed that both high amylose corn and potato starch nanoparticles had granular structure. Potato starch nanoparticles had larger size than nanoparticles of corn starch. These observations were in agreement with DLS data.VD_3-loaded high amylose corn starch nanoparticles. (Fig. 1c) showed formation of V type amylose structure which could be confirmed by XRD results.

Turbidimetry

Turbidimetry is an indirect optical technique for evaluation of nanoparticle aggregates (Gonzalez et al. 2005). Transparency of starch nanoparticles solution was much more than vitamin D_3 loaded nanoparticles (Fig. 2). On the other hand, dispersions of high amylose corn starch nanoparticles were less turbid than potato starch nanoparticles. Absorption of solution of vitamin D_3 in ethanol was almost close to zero and the solution was quite transparent; while turbidity increased by loading of vitamin D_3 in nanoparticles. Increase of turbidity of potato starch nanoparticles was much more than high amylose corn starch nanoparticles. It could be attributed to increase of particle size due to higher load of vitamin D_3 in the potato starch nanoparticles. The results of the turbidimetry were in agreement with DLS data. Dispersions of potato starch nanoparticles in double distilled water during 24 h had more stability to deposition. Transparencies of nanoparticle dispersions in distilled water (concentration of recommended dose of vitamin D_3 for food fortification) were desirable in every 8 formulations and they had capability of being used in clear drinks.

Fourier transform infrared spectroscopy

FTIR analysis was carried out to investigate the interactions between vitamin D_3 and starch. For this purpose, spectrum of high amylose corn starch, potato starch, vitamin D_3, vitamin D_3 loaded nanoparticles that have smaller size and a more favorable load (CSN-0-10 and PSN-0-10) and physical mixture of starches and vitamin D_3 with weight ratio similar to vitamin loaded nanoparticles were investigated.

Major bands at 3419 and 3434 cm^{-1} were observed in the spectra of potato starch and high amylose corn starch, respectively. These peaks were denoted to the stretching of hydrogen-bonded O–H groups. For both starches the unsymmetrical stretching of C–H (CH_2 group) was observed at 2929 cm^{-1}. The absorption band at 1643 cm^{-1} was due to the presence of bonded water in starch. The peak at 1383 cm^{-1} represented the angular deformation of C–H (CH_3 group). Similarly the peak at 987 cm^{-1} was related to the C–O–C of α-1,4 and α-1,6 glycosidic linkages (Shi et al. 2012). Other peaks, at 1160 and 1082 cm^{-1} were associated with C–O bond and C–C bond, which were visible in physical mixture spectra while those were weaker for nanoparticle. Vitamin D_3 had relatively weak hydrogen bonds with a sharp peak at 3292 cm^{-1}. The peaks at 2935 and 2874 cm^{-1} of vitamin D_3 spectra were related to alkyl C–H stretch and several others C–H linkage were noticeable in the range of 1052–1460 cm^{-1}. As can be seen in Fig. 3, sharp peaks of vitamin D_3, which some of them were visible in the physical mixture (around 1460 cm^{-1} (and were not found in the spectrum of vitamin loaded nanocarriers that well confirmed encapsulation of the vitamin D_3 in both starches. The peak around 1460 cm^{-1} was related to C–H vibration bending of the methylene group of vitamin D_3 and after loading of vitamin D_3 in starch this peak was omitted which can be attributed to the van der Waals bond between methylene groups of the vitamin D and hydrogen of carbon five in glucose (Immel and Lichtenthaler 2000). In the spectrum of vitamin D_3 loaded starch nanoparticle, the peaks of C–O–C were shifted from 987 to 1023 and 1020 cm^{-1} for CSN-0-10 and PSN-0-10, respectively. These results indicated the effect of ultrasound on glycoside bonds of starch. For PSN-0-10, peak at 3419 cm^{-1} was shifted to 3400 cm^{-1} after VD_3 loading, suggesting the hydrogen bonding formation between VD_3 and potato starch. Therefore, this bond facilitated encapsulation of VD_3 in potato starch nanoparticles that was in consistent with EE results as discussed earlier.

X-ray diffraction analysis

Crystallography results were depicted in Fig. 4. XRD patterns of high amylose corn starch showed peaks at angles of 17.12, 16.27, and 22.2 (2θ) which were characterized A-type crystalline structure. X-ray diffraction of maize starches did not show any peak at $2\theta = 5.6°$ as observed for potato starch indicating their typical A-pattern (Singh et al. 2006).The diffraction peaks of potato starch an intense peak appeared at 17° (2θ), and other peaks appeared at Bragg angles of 5.6 15, 17, and 23(2θ), which were characterized as B-type crystals (Kim et al. 2012). For pure vitamin D_3 several intense peaks were detected at angles of 7, 12.8, 16.93, and 17.3 which showed its crystal structure. The XRD pattern of the physical mixtures had intensity peaks highly similar to starch and vitamin D_3 and

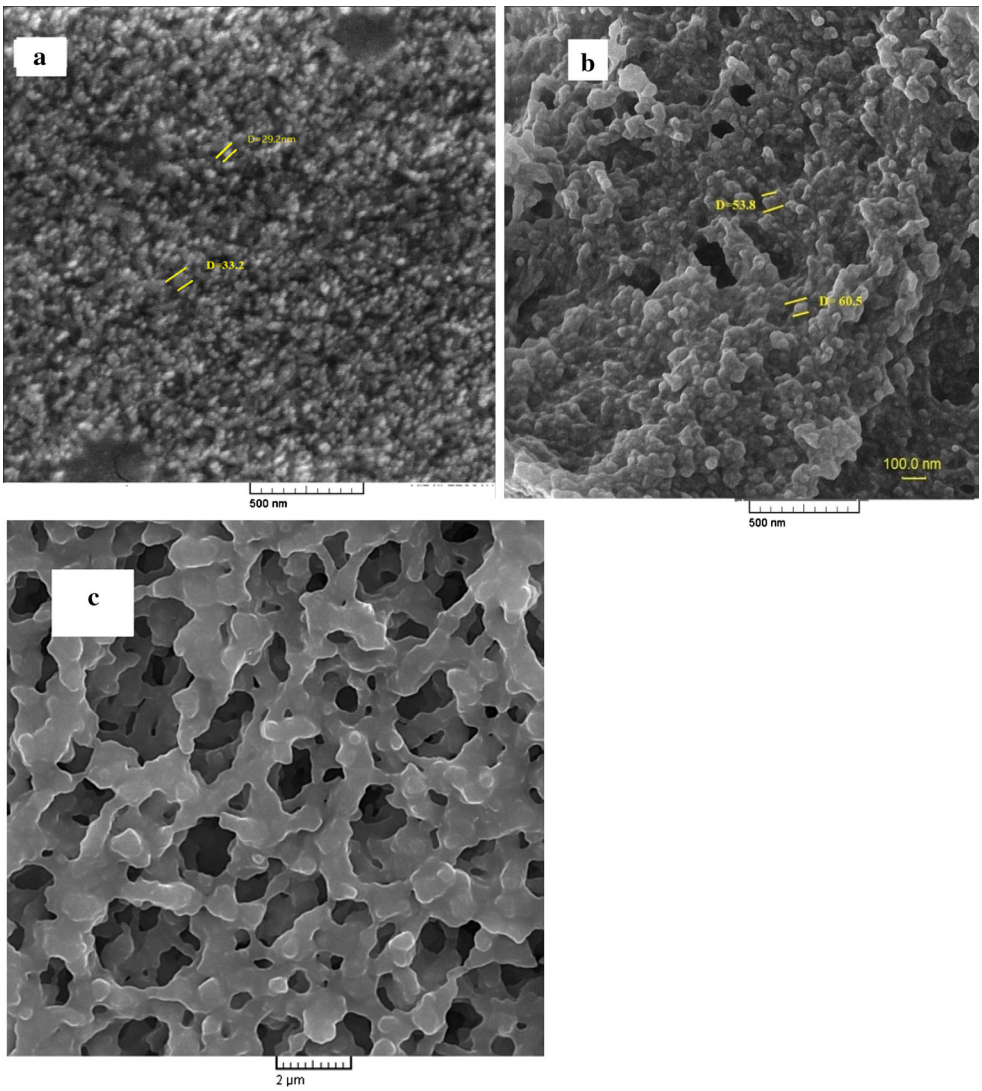

Fig. 1 FE-SEM images of VD-loaded nanoparticles: **a** CSN-0-10, **b** PSN-0-10 and **c** V type amylose structure in VD-loaded high amylose corn starch nanoparticle. [sample code is illustrated starch source—temperature (°C)—time (min)]

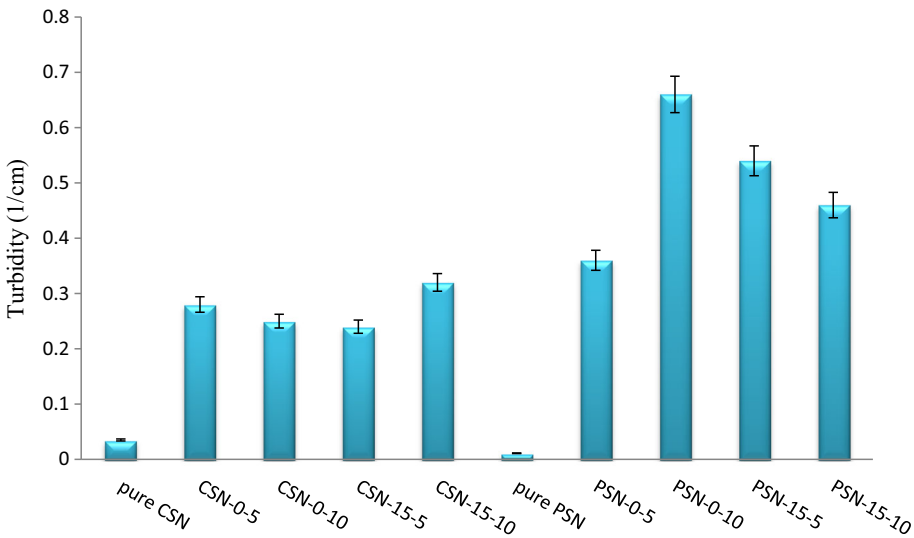

Fig. 2 Mean values of three replications of turbidity of 0.16% (w/v) of different VD_3 loaded nanoparticles and pure nanoparticles solution. [sample code is illustrated starch source—temperature(°C)—time (min)]

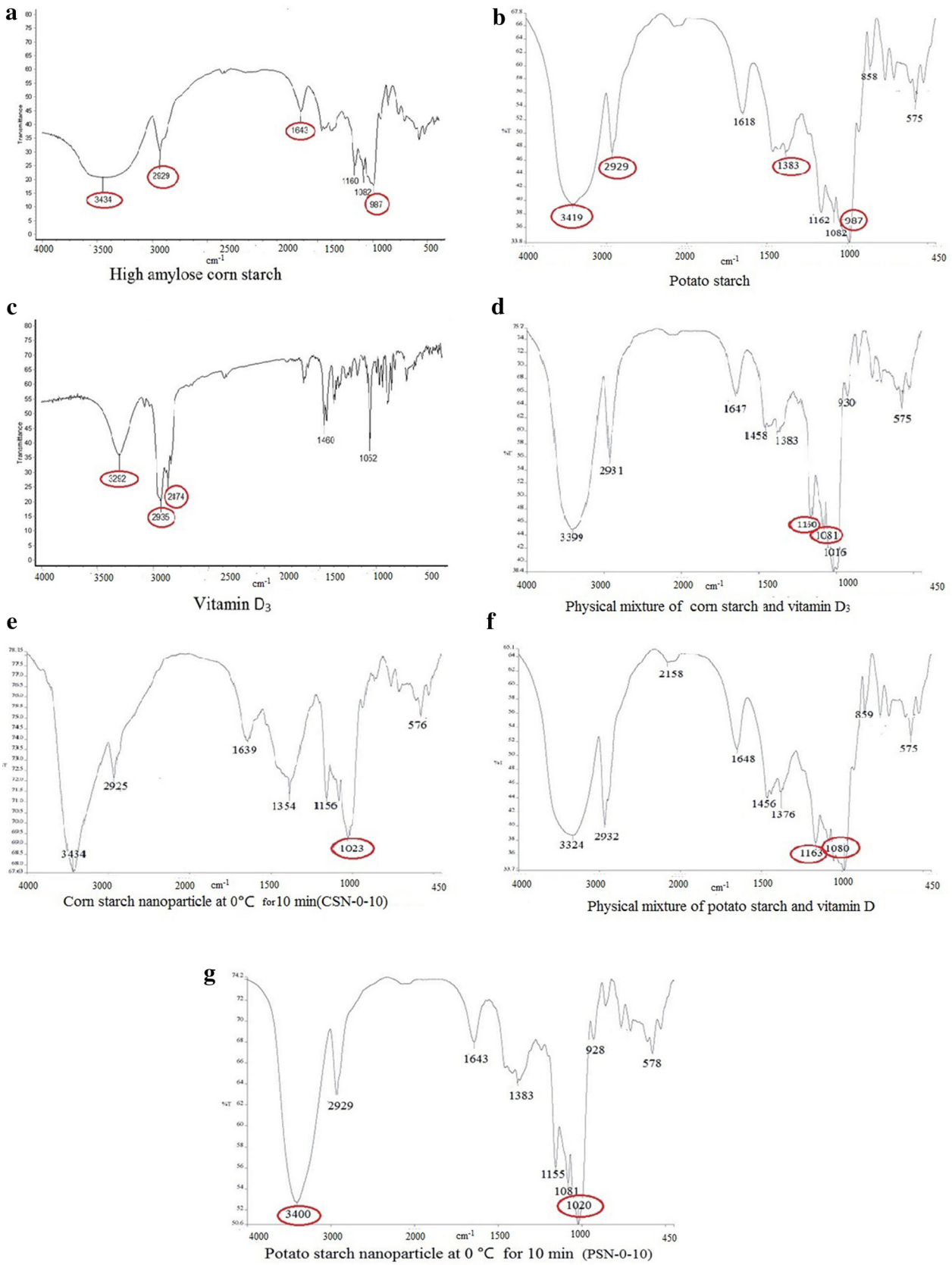

Fig. 3 FTIR spectrum of pure materials and different developed vitamin D loaded nanocarriers

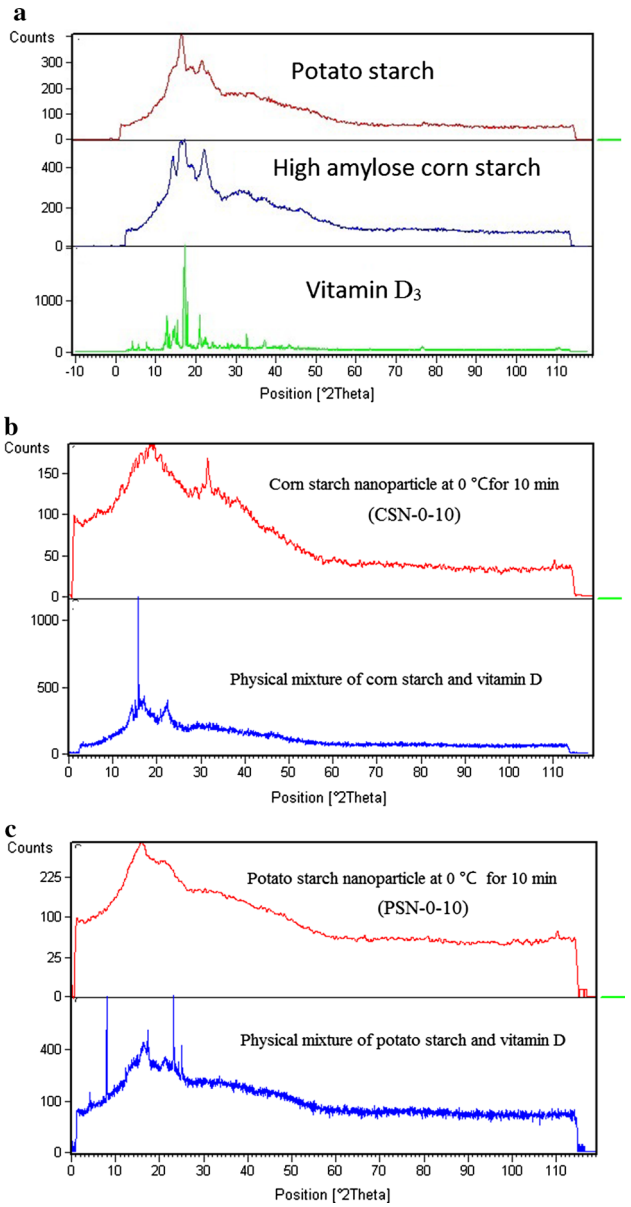

Fig. 4 Diffractograms of pure materials, physical mixtures and developed vitamin D loaded nanocarriers

almost all of peaks can be observed. Comparison of diffraction peaks of starches and the physical mixtures with nanoparticles showed a substantial disruption of the crystalline structure by the ultrasonic treatment. It was assumed that the ultrasonic treatment led to changes in the structure of the starch granules, especially the crystalline regions of amylopectin (Sun et al. 2014). Therefore, increase of EL and EE of potato starch nanoparticles for PSN-0-10 is associated with ultrasonic effect on amylopectin structure (Haaj et al. 2013). Hence, PSN-0-10 had more amorphous structure than CSN-0-10 and potato starch. Intense peaks of vitamin were removed in XRD pattern of vitamin D_3 loaded nanoparticle suggested that vitamin was successfully encapsulated in starch. XRD pattern obtained for potato starch nanocarriers had peaks at Bragg angle of 16.6 and 21.7 while generally exhibited a broad peak in the whole curve that associated with amorphous structure. Nevertheless high amylose corn starch nanocarriers had peaks at Bragg angle of 13.1, 20 and 32. According to previous reports for high amylose corn starch nanocarriers, peaks at Bragg angle of 13.1 and 20 were related to formation of amylose–lipid complex and showed V-type crystalline structure (Xu et al. 2013; Singh et al. 2006). In addition, existence of a peak at Bragg angle of 32 indicated formation of a new crystalline structure in vitamin D_3 loaded high amylose corn starch. However, it should be mentioned that the crystallinity of the nanoparticles is less than used starches and physical mixtures. Temperature increases induced by the ultrasonic treatments might assist decrease of crystallinity (Kim et al. 2013). The results of X-ray diffraction suggested that amylopectin is able to interact with the vitamin D_3. It is conceivable that the side chains of amylopectin form helical inclusion interacting with vitamin D_3. This is in agreement with report of Heinemann et al. (2003) who stated that amylopectin is able to interact with the ò-lactones and the interaction of d-lactone with amylopectin is independent of the botanical origin of the starch.

Thermal properties

DSC thermograms corresponding to HACS, potato starch, VD_3, physical mixture and vitamin D_3 loaded nanoparticles are shown in Fig. 5. Vitamin D_3 showed a sharp peak at 87.8 °C corresponding to its melting point and its crystal structure. Pure potato and high amylose corn starch curves displayed broad endotherm glass transition at vicinities 95 and 86 °C and a sharp endotherm melting transition at 274.7 and 277.2 °C, respectively. The broad glass transition was due to starch amorphous structure and may be due to overlapping of endothermic events at gelation point of amylopectin (Ragab and El-Kader 2013). High amylose corn starch showed lower transition temperatures that may be caused by the presence of a lower crystalline region and as well as gelatinization enthalpy. It has been reported that higher transition temperatures resulted from a higher degree of crystallinity, which provides structural stability and makes the granules more resistant to gelatinization. Starches with long branched chain length in amylopectin molecules displayed higher gelatinization enthalpy, indicating that more energy was required to gelatinize crystallites of long chain length amylopectin (Singh et al. 2008).The physical mixtures showed two endothermic peaks that corresponding to the melting point of vitamin D_3 and starch. Vitamin peak was not observed in the thermograms of nanoparticles that showed appropriate entrapment of vitamin. Change of slope was also observed

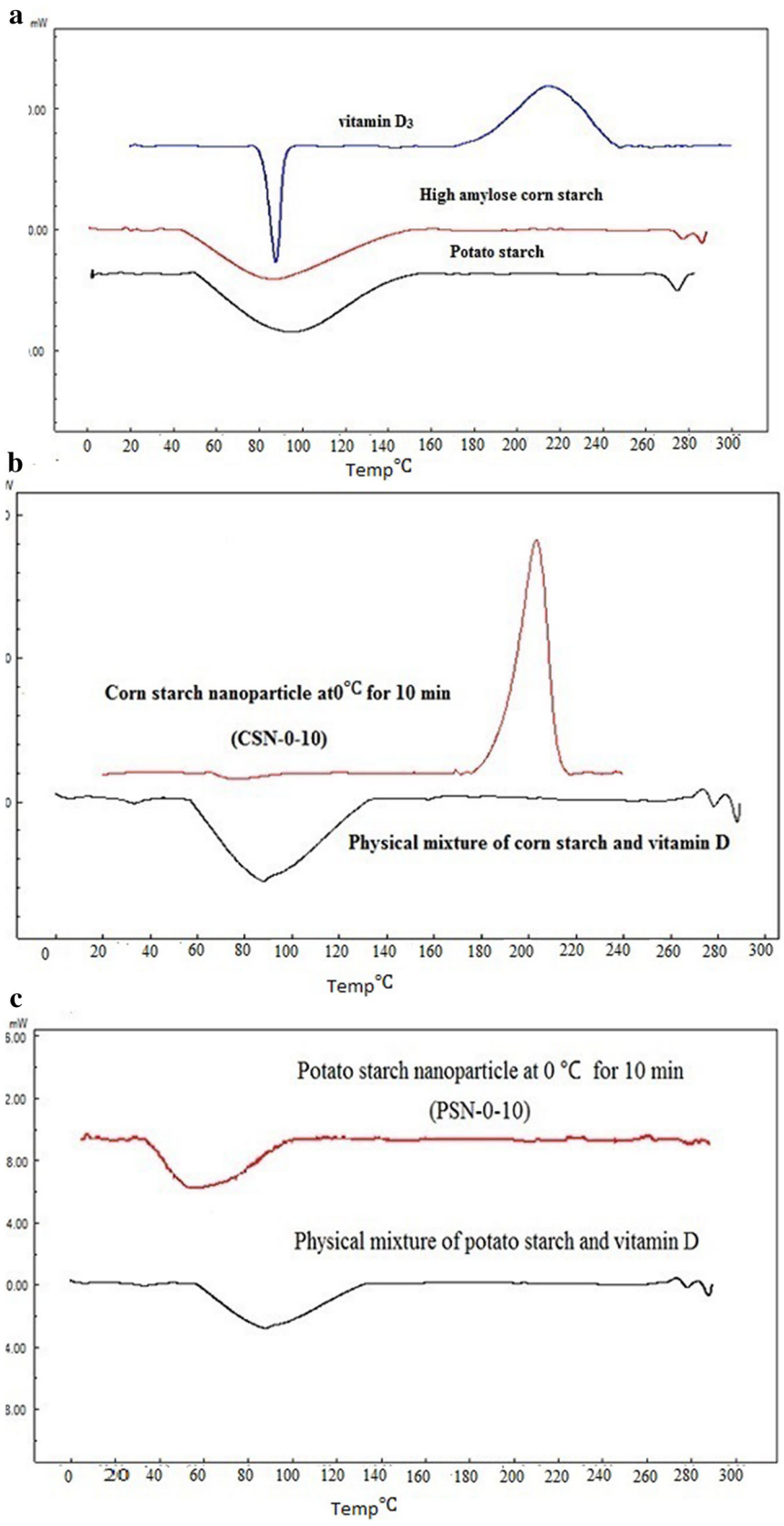

Fig. 5 Thermogram of pure materials, physical mixtures and developed vitamin D loaded nanocarriers

at 57.9 °C (glass transition point) and 211 °C (crystallization temperature) for high amylose corn starch nanoparticle. While only a broad glass transition at 62 °C in DSC thermogram of potato starch nanoparticle was observed and peak of the crystallization temperature was not recognized that indicating these nanoparticles had higher melting point and more amorphous structure which was confirmed by XRD results. Glass transition temperature and crystallinity for treatment PSN-0-10 was lower than its physical mixture which indicating structure destruction by ultrasound treatment. Ultrasonic treatment led to increase of hydrocarbon chain that resulted in van der Waals and hydrogen bonds of vitamin D_3 with the potato starch and greater stability and higher melting temperature. Similar results obtained by Itthisoponkul et al. (2007) for fatty acids and alcohols. They reported when the hydroxyl group is located far from the first carbon atom, melting temperature decreased which could indicate that the position of the hydroxyl group had an effect on the formation and stability of the amylose complex. There are more intermolecular interactions in the crystalline state which are hydrogen bonding between adjacent helices. Therefore more energy is needed to melt the crystal.

Conclusion

Vitamin D_3-loaded nanoparticles were developed by two types of starches with different amylose to amylopectin ratios (high amylose corn and potato starches) and their physicochemical properties were studied using FE-SEM, FRIR, XRD and DSC. All carriers had nano-size range with negative zeta potential. Omission of sharp peak of vitamin D_3 in FTIR spectrum of vitamin loaded nanocarriers and reduction of crystallinity of produced nanocarriers in comparison to pure materials in XRD patterns indicated that vitamin D_3 was successfully entrapped in both starches. In addition to formation of van der Waals bonds, hydrogen bonds are also responsible of enhancement of encapsulation efficiency for potato starch with a low amylose to amylopectin ratio. It could be concluded that although potato starch nanoparticles showed larger size, while due to high encapsulation efficiency and load, and zeta potential, might be preferred for large scale production.

References

Almouazen E, Bourgeois S, Jordheim LP, Fessi H, Briançon S (2013) Nano-encapsulation of vitamin D_3 active metabolites for application in chemotherapy: formulation study and in vitro evaluation. Pharm Res 30(4):1137–1146

Araújo MA, Cunha AM, Mota M (2004) Enzymatic degradation of starch-based thermoplastic compounds used in protheses: identification of the degradation products in solution. Biomaterials 25(13):2687–2693

Bhosale RG, Ziegler GR (2010) Preparation of spherulites from amylose–palmitic acid complexes. Carbohydr Polym 80(1):53–64

Boutboul A, Giampaoli P, Feigenbaum A, Ducruet V (2002) Influence of the nature and treatment of starch on aroma retention. Carbohydr Polym 47(1):73–82

Davis JP, Supatcharee N, Khandelwal RL, Chibbar RN (2003) Synthesis of novel starches in planta: opportunities and challenges. Starch-Stärke 55(3–4):107–120

Esfanjani AF, Jafari SM, Assadpoor E, Mohammadi A (2015) Nano-encapsulation of saffron extract through double-layered multiple emulsions of pectin and whey protein concentrate. J Food Eng 165:149–155

Godet M, Bizot H, Buléon A (1995) Crystallization of amylose—fatty acid complexes prepared with different amylose chain lengths. Carbohydr Polym 27(1):47–52

Gökmen V, Mogol BA, Lumaga RB, Fogliano V, Kaplun Z, Shimoni E (2011) Development of functional bread containing nanoencapsulated omega-3 fatty acids. J Food Eng 105(4):585–591

Gonzalez VD, Gugliotta LM, Vega JR, Meira GR (2005) Contamination by larger particles of two almost-uniform latices: analysis by combined dynamic light scattering and turbidimetry. J Colloid Interface Sci 285(2):581–589

Guichard E (2002) Interactions between flavor compounds and food ingredients and their influence on flavor perception. Food Rev Int 18(1): 49–70

Haaj SB, Magnin A., Pétrier C, Boufi S (2013) Starch nanoparticles formation via high power ultrasonication. Carbohydr polymers 92(2):1625–1632

Hasanvand E, Fathi M, Bassiri A, Javanmard M, Abbaszadeh R (2015) Novel starch based nanocarrier for vitamin D fortification of milk: production and characterization. Food Bioprod Process 96:264–277

Heinemann U, Kiziak C, Zibek S, Layh N, Schmidt M, Griengl H, Stolz A (2003) Conversion of aliphatic 2-acetoxynitriles by nitrile-hydrolysing bacteria. Appl Microbiol Biotechnol 63(3):274–281

Heinemann C, Zinsli M, Renggli A, Escher F, Conde-Petit B (2005) Influence of amylose-flavor complexation on build-up and breakdown of starch structures in aqueous food model systems. LWT-Food Sci Technol 38(8):885–894

Immel S, Lichtenthaler FW (2000) The hydrophobic topographies of amylose and its blue iodine. Flex Rigid Non-glucose Cyclooligosaccharides: Synth Struct Prop 52(1):27

Itthisoponkul T, Mitchell JR, Taylor AJ, Farhat IA (2007) Inclusion complexes of tapioca starch with flavour compounds. Carbohydr Polym 69(1):106–115

Jiang Y, Petrier C, Waite TD (2006) Sonolysis of 4-chlorophenol in aqueous solution: effects of substrate concentration, aqueous temperature and ultrasonic frequency. Ultrason Sonochem 13(5):415–422

Kim HY, Lee JH, Kim JY, Lim WJ, Lim ST (2012) Characterization of nanoparticles prepared by acid hydrolysis of various starches. Starch-Stärke 64(5):367–373

Kim H-Y, Han J-A, Kweon D-K, Park J-D, Lim S-T (2013) Effect of ultrasonic treatments on nanoparticle preparation of acid-hydrolyzed waxy maize starch. Carbohydr Polym 93(2):582–588

Luo Y, Teng Z, Wang Q (2012) Development of zein nanoparticles coated with carboxymethyl chitosan for encapsulation and controlled release of vitamin D_3. J Agric Food Chem 60(3):836–843

Makino K, Mossoba MM, Riesz P (1983) Chemical effects of ultrasound on aqueous solutions. Formation of hydroxyl radicals and hydrogen atoms. J Phys Chem 87(8):1369–1377

Merisko-Liversidge EM, Liversidge GG (2008) Drug nanoparticles: formulating poorly water-soluble compounds. Toxicol Pathol 36(1):43–48

Patist A, Bates D (2008) Ultrasonic innovations in the food industry: from the laboratory to commercial production. Innov Food Sci Emerg Technol 9(2):147–154

Pettifor JM, Prentice A (2011) The role of vitamin D in paediatric bone health. Best Pract Res Clin Endocrinol Metab 25(4):573–584

Putseys J, Lamberts L, Delcour J (2010) Amylose-inclusion complexes: formation, identity and physico-chemical properties. J Cereal Sci 51(3):238–247

Ragab H, El-Kader MA (2013) Optical and thermal studies of starch/methylcellulose blends. Phys Scr 87(2):025602

Rao KS, El-Hami K, Kodaki T, Matsushige K, Makino K (2005) A novel method for synthesis of silica nanoparticles. J Colloid Interface Sci 289(1):125–131

Relkin P, Shukat R (2012) Food protein aggregates as vitamin-matrix carriers: impact of processing conditions. Food Chem 134(4):2141–2148

Ron N, Zimet P, Bargarum J, Livney Y (2010) Beta-lactoglobulin–polysaccharide complexes as nanovehicles for hydrophobic nutraceuticals in non-fat foods and clear beverages. Int Dairy J 20(10):686–693

Shi A-M, Wang L-J, Li D, Adhikari B (2012) The effect of annealing and cryoprotectants on the properties of vacuumfreeze dried starch nanoparticles. Carbohydr Polym 88(4):1334–1341

Singh N, Inouchi N, Nishinari K (2006) Structural, thermal and viscoelastic characteristics of starches separated from normal, sugary and waxy maize. Food Hydrocoll 20(6):923–935

Singh N, Isono N, Srichuwong S, Noda T, Nishinari K (2008) Structural, thermal and viscoelastic properties of potato starches. Food Hydrocoll 22(6):979–988

Sun Q, Fan H, Xiong L (2014) Preparation and characterization of starch nanoparticles through ultrasonic-assisted oxidation methods. Carbohydr Polym 106:359–364

Suslick KS (1988) Ultrasound: its chemical, physical, and biological effects. VCH Publishers, Weinheim

Teng Z, Luo Y, Wang Q (2013) Carboxymethyl chitosan–soy protein complex nanoparticles for the encapsulation and controlled release of vitamin D_3. Food Chem 141(1):524–532

Tischer PCF, Sierakowski MR, Westfahl H Jr, Tischer CA (2010) Nanostructural reorganization of bacterial cellulose by ultrasonic treatment. Biomacromol 11(5):1217–1224

Üner M (2006) Preparation, characterization and physico-chemical properties of solid lipid nanoparticles (SLN) and nanostructured lipid carriers (NLC): their benefits as colloidal drug carrier systems. Die Pharm Int J Pharm Sci 61(5):375–386

Xu J, Zhao W, Ning Y, Bashari M, Wu F, Chen H, Zhang L (2013) Improved stability and controlled release of ω3/ω6 polyunsaturated fatty acids by spring dextrin encapsulation. Carbohydr Polym 92(2):1633–1640

Zuo YYJ, Hébraud P, Hemar Y, Ashokkumar M (2012) Quantification of high-power ultrasound induced damage on potato starch granules using light microscopy. Ultrason Sonochem 19(3):421–426